

Stability of metallic stripes in the extended one-band Hubbard model

G. Seibold¹ and J. Lorenzana²

¹*Institut für Physik, BTU Cottbus, PBox 101344, 03013 Cottbus, Germany*

²*Center for Statistical Mechanics and Complexity, INFN, Dipartimento di Fisica, Università di Roma La Sapienza, P. Aldo Moro 2, 00185 Roma, Italy*

(Dated: November 23, 2018)

Based on an unrestricted Gutzwiller approximation (GA) we investigate the stripe orientation and periodicity in an extended one-band Hubbard model. A negative ratio between next-nearest and nearest neighbor hopping t'/t , as appropriate for cuprates, favors partially filled (metallic) stripes for both vertical and diagonal configurations. At around optimal doping diagonal stripes, site centered (SC) and bond centered (BC) vertical stripes become degenerate suggesting strong lateral and orientational fluctuations. We find that within the GA the resulting phase diagram is in agreement with experiment whereas it is not in the Hartree-Fock approximation due to a strong overestimation of the stripe filling. Results are in agreement with previous calculations within the three-band Hubbard model but with the role of SC and BC stripes interchanged.

PACS numbers: 71.28.+d, 71.10.-w, 74.72.-h, 71.45.lr

I. INTRODUCTION

The existence of stripes, i.e. antiphase domain walls in an antiferromagnet stabilized by doped holes, is now a well established fact in cuprate^{1,2,3,4,5,6} and nickelate^{7,8,9} materials.

Direct evidence for static stripes in cuprates has been more clearly established in $\text{La}_{2-x}\text{Sr}_x\text{CuO}_4$ (LSCO) eventually co-doped with Nd or Eu. However incommensurate inelastic neutron scattering signals (widely interpreted as evidence for dynamical stripe fluctuations) have been found in both LSCO and $\text{YBa}_2\text{Cu}_3\text{O}_{7-\delta}$ (YBCO) compounds with a remarkably similar phenomenology.¹⁰ Even more static charge order has been found in YBCO without the need for additions like Nd.¹¹

In LSCO the inverse stripe spacing grows linearly with doping x up to $x \approx 1/8$ and the orientation rotates from vertical (i.e. oriented along the Cu-O bonds) by 45° to diagonal for concentrations lower $x \approx 0.05$.^{4,12,13} Moreover, from this linear relation it turns out that in the LSCO compounds stripes are characterized by one doped hole per two unit cells along the domain wall, that is a linear density of added holes $\nu \approx 0.5$ (hereafter called 'half-filled stripe').

Regarding the $\text{Bi}_2\text{Sr}_2\text{CaCu}_2\text{O}_8$ (BiSCCO) family it is a very difficult material to perform neutron scattering so few experiments exist [see the discussion in Ref. 14]. Interestingly this study finds a peak much broader than the momentum resolution leaving plenty of room for incommensurate effects. The existence of incommensurate scattering in BiSCCO is also supported by the experiments of Ref. 15. While most neutron scattering experiments focus on the structure of spin excitations, the inhomogeneous charge distribution as arising from the formation of stripes has also been detected by local probes like NQR^{16,17} and NMR.¹⁸ Due to refinements in the experimental technique Haase et al.¹⁸ were even able to demonstrate a correlation of charge and density variations on short length scales.

All these experiments suggest that stripes are a common phenomena of all cuprates families and therefore may be related to superconductivity.

Concerning the theoretical aspects, stripes were predicted by the inhomogeneous Hartree-Fock (HF) approximation in the three-band Hubbard model¹⁹, the one-band Hubbard^{20,21} and the $t-J$ model.²² However these pioneering studies predicted insulating stripes with a linear density of $\nu = 1$ added holes per lattice constant along the stripe (instead of $\nu \sim 0.5$) which led to an early rejection of stripes.²³

Recently we have presented a computation of metallic mean-field stripes²⁴ within an unrestricted Gutzwiller approximation²⁵ (GA) applied to the three-band Hubbard model. The behavior of the magnetic incommensurability $\epsilon \equiv 1/(2d)^{3,4,5,6}$ (d is the distance between charged stripes in units of the lattice constant), chemical potential^{26,27}, and transport experiments^{28,29} as a function of doping has been explained in a parameter free way.²⁴ Addition of RPA-type fluctuations within a recently developed time dependent GA³¹ has explained³² also the evolution of the optical conductivity with doping^{33,34} in a broad frequency range.

In our previous computations^{24,32} we fixed the parameter set of the three band Hubbard model to the values derived for the LSCO family within the local density approximation (LDA).³⁵ In this sense we view our previous work as the last stage of an *ab initio* determination of the electronic structure. On the contrary we would like to explore in the present paper the parameter dependence of the results. This kind of investigation is interesting not only in order to check the robustness of the results but also to obtain hints about the expected trends in the behavior among the different cuprates materials. The complexity of the three band model, however, makes it difficult to perform such study. To achieve our goals we adopt here a much simpler Hamiltonian, namely the extended one-band Hubbard model. Given the popularity of the model it is also interesting to explore, to what ex-

tent the physics found in the three band Hubbard model can be found in the one band counterpart. In the present work we find that for realistic parameters a similar phase diagram is found in the one-band and the three-band models²⁴ however some important details about the symmetry of stripes differ.

Regarding the material dependence it has been proposed recently³⁶ that a one-band model description of the various cuprate families essentially differs in the ratio between next-nearest and nearest neighbor hopping t'/t . In fact it is found that the transition temperature scales with t'/t ranging from $t'/t \approx -0.15$ for the LSCO single layer compound up to $t'/t \approx -0.4$ for the Tl and Hg based materials. We show that this parameter plays a key role for the stability and electronic structure of the stripes suggesting a possible connection between stripes and superconductivity. In particular the higher the t' the smaller is the optimum filling ν of the stripe (Fig. 6). Additionally we present a thorough comparison of the stability of stripe and polaron textures upon varying t'/t .

The influence of a next-nearest neighbor hopping term on the stripe formation has been previously investigated by dynamical mean-field theory (DMFT)³⁷ and the HF approximation.^{38,39,40} It was found^{40,41} that increasing the ratio $|t'/t|$ leads to a suppression of static stripes. This may indicate a more dynamical character of stripes in some systems like Tl and Hg based compounds.

In case of the HF approximation⁴³ vertical stripe solutions are only favored for unrealistic small values of $U/t \approx 3...5$ whereas a ratio of $U/t \approx 10$ is required in order to reproduce the low energy spectrum of the three-band model.⁴⁴ Therefore our investigations here are based on the unrestricted Gutzwiller approximation⁴⁵ which provides an excellent variational Ansatz for the ground state energy of the Hubbard model. We compare our results with the HF approximation and show that HF cannot account for the site centered stripe topology as relevant in the one-band model.

In Sec. II we briefly outline our method and present the results of our calculation in Sec. III. Finally we conclude the discussion in Sec. IV.

II. MODEL AND FORMALISM

We consider the two-dimensional Hubbard model on a square lattice, with hopping restricted to nearest ($\sim t$) and next nearest ($\sim t'$) neighbors

$$H = -t \sum_{\langle ij \rangle, \sigma} c_{i, \sigma}^\dagger c_{j, \sigma} \quad (1)$$

$$- t' \sum_{\langle\langle ij \rangle\rangle, \sigma} c_{i, \sigma}^\dagger c_{j, \sigma} + U \sum_i n_{i, \uparrow} n_{i, \downarrow}.$$

Here $c_{i, \sigma}^{(\dagger)}$ destroys (creates) an electron with spin σ at site i , and $n_{i, \sigma} = c_{i, \sigma}^\dagger c_{i, \sigma}$. U is the on-site Hubbard repulsion which in the following is fixed to the value $U/t = 10$ as

relevant for the cuprates (see e.g. Refs. 44,46). The unrestricted Gutzwiller approximation (GA) can be implemented by either a variational Ansatz⁴⁷ or the Kotliar-Ruckenstein slave-boson scheme⁴⁸ and results in the following energy functional

$$E^{GA}(\rho, D) = -t \sum_{\langle ij \rangle, \sigma} z_{i, \sigma}^{GA} z_{j, \sigma}^{GA} \rho_{ij, \sigma} \quad (2)$$

$$- t' \sum_{\langle\langle ij \rangle\rangle, \sigma} z_{i, \sigma}^{GA} z_{j, \sigma}^{GA} \rho_{ij, \sigma} + U \sum_i D_i$$

where $\rho_{ij, \sigma} = \langle c_{i, \sigma}^\dagger c_{j, \sigma} \rangle$ denotes the single-particle density matrix, D_i are variational parameters related to the double occupancy of the sites and the Gutzwiller hopping factors are given by

$$z_{i, \sigma}^{GA} = \frac{\sqrt{(1 - \rho_{ii} + D_i)(\rho_{ii, \sigma} - D_i)} + \sqrt{D_i(\rho_{ii, -\sigma} - D_i)}}{\sqrt{\rho_{ii, \sigma}(1 - \rho_{ii, \sigma})}}. \quad (3)$$

The energy functional Eq. (2) has to be minimized with respect to the double occupancy parameters D and the density matrix ρ where the latter variation has to be constrained to the subspace of Slater determinants. For technical aspects of this variational procedure we refer to Ref. 45.

The clusters investigated in the following have dimensions $N = N_x \times L$ up to 16×16 and we use periodic and antiperiodic boundary conditions in order to stabilize homogeneous (metallic) stripe textures.

III. RESULTS

A. Charge and spin profile of stripes

In Fig. 1 we report the typical charge- and spin profiles in a cut perpendicular to the stripe for vertical site (SC) and bond (BC) centered stripes as computed with HF and GA respectively. All vertical stripe solutions investigated in this paper are metallic (i.e. homogeneous along the stripe) except for integer ν and we have suppressed 1-D instabilities by choosing appropriate boundary conditions (i.e. periodic or antiperiodic in direction of the stripes).

The total charge shows dips at the central site (sites) of the antiphase SC (BC) domain walls (Fig. 1a,d) corresponding to the accumulation of holes. As also found in previous studies^{24,45,49} the GA charge modulation is much weaker as compared to HF.

Due to symmetry of the antiphase domain walls the spin density is zero along the stripe in case of SC stripes (Fig. 1a-c). Therefore a large charge reduction is the only possibility to reduce the HF double occupancy on these sites. On the other hand the double occupancy within the GA can be separately tuned by the variational parameter D leading to a smaller charge modulation amplitude with respect to HF. In Fig. 1c we show the smaller

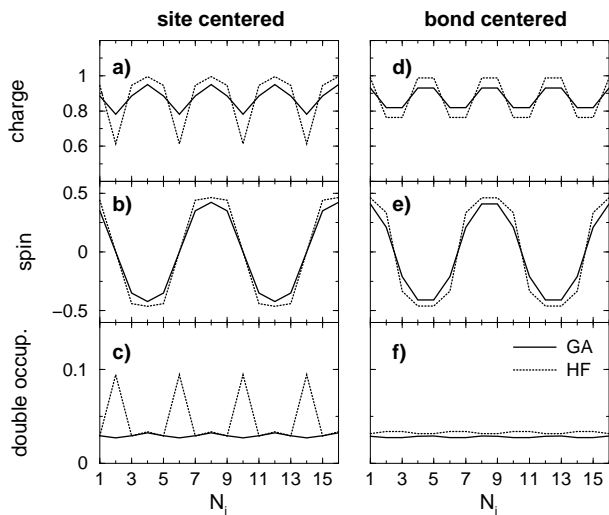


FIG. 1: Profile of the charge density (a,d), staggered spin order parameter (b,e), and double occupancy (c,f) of site centered (a-c) and bond centered (d-f) stripes. Results are for $t'/t = -0.2$ and $n_s = 4$ half-filled stripes on a 16×16 lattice corresponding to $d = 4$ and $x = 1/8$.

double occupancy at the core stripes sites (like site 2) for the GA whereas both HF and GA acquire approximately the same value within the AF ordered regions. In contrast, the BC stripe solution has finite spin polarization on all sites (Fig. 1e) so that in this case a large HF double occupancy is avoided (Fig. 1f). This has important consequences for the respective stability of BC and SC stripes within the two approximations as we will see below.

B. Effect of t' on the band structure

In order to understand the role of t' in the context of stripe formation we proceed by investigating the influence of this parameter on the electronic structure. Within our variational (mean-field) approach the undoped system is characterized by a homogeneous spin-density wave state which band structure is characterized by a lower (filled) and an upper (empty) Hubbard band, separated by a single particle energy gap Δ . Due to the incorporation of correlation effects already on the mean-field level, Δ^{GA} is significantly smaller than within the HF approximation where it is simply given by $\Delta^{HF} = Um$ and m denotes the magnetic moment.

The stripe state at finite doping induces the formation of two bands within the Mott-Hubbard gap. These are almost flat perpendicular to the stripes but some dispersion develops when the stripes become closer, similar to what is found in the 3-band model.²⁴ In Fig. 2 we show the dispersion for both bands in the stripe direction (y) for various values of t'/t .

Doped holes occupy states in the lower band (here-

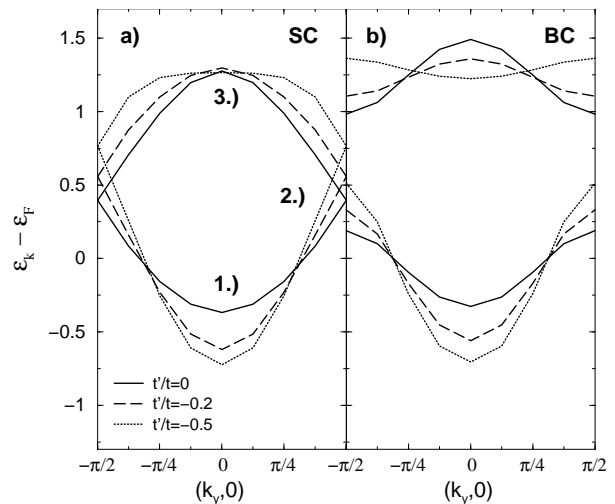


FIG. 2: Dispersion of the mid-gap bands along vertical $d = 4$ stripes in a 16×16 lattice computed within the GA. $t'/t = 0, -0.2, -0.5$. a) Site centered stripes; b) Bond centered stripes

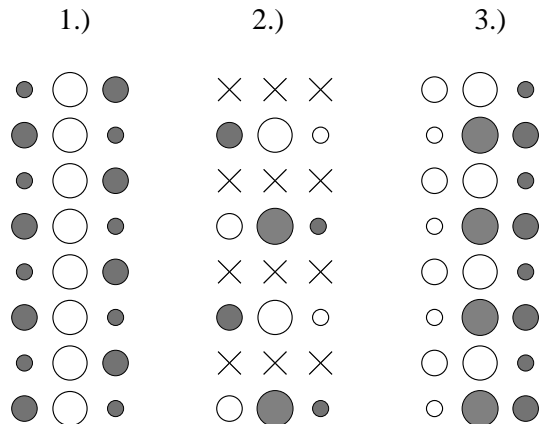


FIG. 3: Sketch of the amplitudes $\Phi_i(k)$ along site centered stripe sites i for selected k -states as indicated in the band structure of Fig. 2a. 1.) $\equiv k = (0, 0)$ of the active band; 2.) $\equiv k = (\pi/2, 0)$; 3.) $\equiv k = (0, 0)$ of the upper band. Empty (full) circles correspond to positive (negative) amplitudes which value is indicated by the radius. Crosses mark $\Phi_i(k) = 0$.

after called the active band) and a half-filled stripe corresponds to a half-filled active band. Furtheron the band-structure of the BC solution (Fig. 2b) displays a gap between both bands which is due to a AF spin-density modulation along the BC stripe. For both, SC and BC stripes, Fig. 2 reveals a significant broadening of the active band upon increasing $|t'|$. This broadening has a strong influence on the kinetic energy of holes in the stripe and therefore also on the density of states at the Fermi energy and, as we will show below, on the value of the optimum ν .

The broadening can be understood by looking at the

single particle wave functions (WF) of selected k-points of the active band as shown in Fig. 3 for the case of SC stripes. The $k = 0$ WF is characterized by having opposite sign at the core of the stripe than on the adjacent (AF ordered) legs. As a consequence a positive next-nearest neighbor hopping (i.e. negative t' , cf. Eq. (1)) leads to a lowering of this state in first order perturbation theory. By the same argument one can show that the zone boundary state of the active band is not affected by t' since next-nearest neighbor hopping along the stripe always connects to a site i with a node in the single particle wave function (the shift in energy in Fig. 2 is due to the fact that E_F shifts downwards with t'). For a sizeable SDW gap Δ on the adjacent legs of the stripe the broadening of the active band can be evaluated as $\delta B = 36t't^2/\Delta^2$. Since $\Delta^{HF} > \Delta^{GA}$ as already mentioned above, the t' band width renormalization is expected to be larger in the GA as compared to HF.

For completeness we mention that similar considerations also hold for the upper band in the Mott-Hubbard gap. From the structure of the $k = (0, 0)$ wave-function (cf. Fig. 2) it turns out that a negative t' induces a shift of this state to lower energies (in Fig. 2 this shift is almost compensated by the change in the chemical potential). Correspondingly we find a narrowing of the upper band $\delta B = -28t't^2/\Delta^2$ which for large t' leads to the flat structure as observed in Fig. 2.

C. Parametrization of e_h ; GA vs. HF

To determine the more stable solution among different textures we need to compare the total energies per atom, E/N , for the same doping, $x \equiv N_h/N$. Equivalently we can compare the excess energy per hole with respect to the undoped antiferromagnet (AF), hereafter the “energy per hole”:

$$e_h = \frac{E(N_h) - E_{AF}}{N_h} \quad (4)$$

where $E(N_h)$ is the total energy of the inhomogeneous state (generally a stripe state) with N_h holes counted from half-filling and E_{AF} is the AF solution on the same cluster. The minimum of e_h at low doping (non-interacting stripes) has the following meaning: it determines the optimum filling that stripes should have in order to accommodate a given number of holes in a variable number of stripes.

In Fig. 4 we report the energies per hole for different configurations in the HF and in the GA approximations as a function of the stripe filling $\nu = N_h/(n_s L)$. Here L is the linear dimension in the y direction of the cluster which coincides with the stripe length, n_s denotes the number of stripes and N_h is the total number of holes (counted from half-filling) in the system. More detailed results for vertical SC and diagonal stripes in the GA are reported in Fig. 5.

In order to analyze these results we expand the excess energy per unit length as a Taylor series in ν :

$$\frac{E(N_h) - E_{AF}}{L} = A + B\nu + C\nu^2. \quad (5)$$

The energy per hole in a stripe thus follows the relation

$$e_h = A/\nu + B + C\nu \quad (6)$$

which provides an excellent fit to the data points as shown in Figs. 4b, 5. The minimum of e_h is given by

$$\nu_{min} = \sqrt{A/C}$$

and the second derivative of the energy per hole at the minimum reads as

$$e_h''(\nu_{min}) = 2C\sqrt{C/A}. \quad (7)$$

Note, however, that the single particle spectrum has a gap for $\nu = 1$. Therefore the energy has a cusp-like singularity at this filling which causes the $\nu = 1$ state to be the minimum for a wide range of parameters. We can take this into account by modifying the above formula to:

$$\nu_{min} = \min(\sqrt{A/C}, 1) \quad (8)$$

In the dilute limit, corresponding to large stripe separation, the coefficients can be interpreted as follows: A is the energy cost per unit length to create an antiphase domain wall in the *stoichiometric* (otherwise AF ordered) system. The parameter B can be defined as the chemical potential to add one hole into the “empty” stripe. Finally the parameter $C = C_K + C_I$ is related to the kinetic (C_K) and interaction (C_I) energy of the system.

In order to separate the two contributions C_K , C_I to the parameter C we have adopted the following procedure. For a small value of ν we have optimized the variational parameters of the GA. Then the energy as a function of ν has been computed *without* changing the variational parameters, i.e. by solely filling the frozen bands. The resulting quadratic contribution to the energy gives the C_K parameter and since C is known we also obtain C_I . Within mean-field the latter is due to readjustments of the charges and double occupancies in response to the added holes.

For the parameters under consideration we find that C_I is approximately 2–3 times larger than C_K . However, it is important to note that C_I is almost independent from the next-nearest neighbor hopping, whereas from Fig. 2 it is obvious that the kinetic energy of the holes moving along the stripe will have a significant dependence on t' . To see more explicitly how the active bandwidth reflects on the kinetic energy one can approximate the active band density of states per spin by a rectangular shape of height $1/W(t')$. Here $W(t')$ represents an effective bandwidth which is roughly given by the width of the lower (active) band in Fig. 2. One finds that the kinetic energy

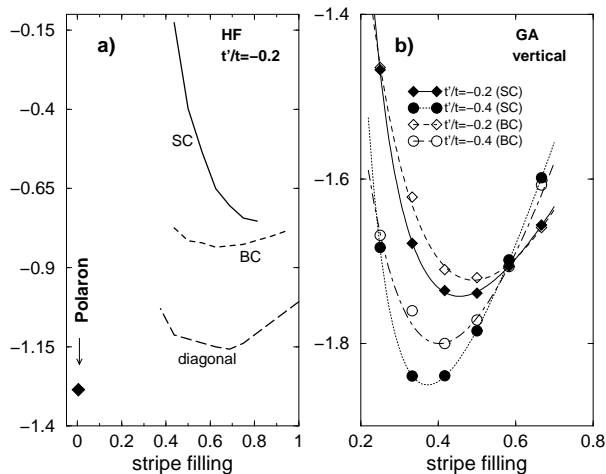


FIG. 4: (a) HF energy per hole e_h for vertical stripes as a function of the stripe filling ν and for various values of t'/t . Results in (a) are for $2d = 5$ stripes on a 10×10 lattice. (b) GA energy per hole for 4 site centered (SC) and bond centered (BC) stripes on a 12×12 lattice (symbols). The lines correspond to fits obtained with Eq. (6)

is quadratic in ν and $C_K \sim W(t')$. Below we discuss in detail how t' determines the stability of stripes via this mechanism.

To estimate A we need an estimate of the energy to create an empty domain wall. Since this is related to an excitation of the undoped system we can use the Heisenberg model with a magnetic interaction $J = 4t^2/U$ in the limit of $U \gg t$. The estimate is easily done in the case of BC stripes which have a core with ferromagnetic alignment along the domain wall. In the Néel limit one obtains: $A = J/2$.

The case of SC stripes is more subtle. Indeed for SC stripes one has a core without permanent moments which, contrary to the BC case, does not have a classical analog within a Heisenberg description of the undoped state. A non classical state will consist of a spin liquid along the core which in any case will give $A \sim J$. Within the HF approximation of the Hubbard model the corresponding solution has a non-magnetic core with maximum double occupancy ($1/4$). This is at odds with the Heisenberg picture of a spin liquid core which, by construction, implies small double occupancy for the original fermions. Therefore the HF approximation introduces an error in A which in the large U limit is of the order of $U/4$. This is due to the fact that moment formation is the only mechanism within HF to reduce double occupancy. On the other hand the GA allows an unpolarized state with small double occupancy ($D \sim t^2/U^2$) thanks to the additional variational parameters D_i as shown in Fig. 1c,f. Due to this mechanism we obtain A within the GA of the correct order $A \sim UD \sim J$. We see in Fig. 4 that the curves for SC and BC stripes are similar in the GA whereas in HF metallic SC stripes are energetically unfavorable with respect to BC (and diagonal) ones.

Clearly the latter faultiness of the HF approach is due to the overestimation of the parameter A mentioned above [c.f. Eq. 8] which leads to an unphysical large value of ν_{min} . For this reason we conclude that HF theory is not an adequate approach for the description of SC stripes.

Within the HF approximation it is known⁴³ that for $U/t > 3.6$ vertical stripes are less stable than diagonal ones. Moreover spin polarons become the ground state when $U/t > 8$. Fig. 4a demonstrates that similar results hold when one includes next-nearest neighbor hopping. As we will show below the situation is quite different in the GA approximation which also allows a comparison between SC and BC stripes on an equal footing.

It is seen from Fig. 4b that within the Gutzwiller approach SC stripes become degenerate with BC for large and small filling factors ν . Especially it turns out that BC empty stripes are slightly lower in energy than SC empty stripes. However, SC stripes tend to have larger bandwidth than BC ones (cf. Fig. 2) which leads to a larger C , larger curvatures of e_h vs. ν [Eq. (7)] and hence smaller values of ν . The difference in curvature allows for the two intersections between the e_h curves for BC and SC solutions in Fig. 4b. We will show below that the crossing at large ν corresponds to optimal doping and that in the underdoped case SC stripes are more stable than BC ones. The stability of SC solutions with respect to BC ones at low doping as well as the increased degeneracy for larger concentration is in agreement with DMFT calculations in the one-band model.⁵² Therefore it seems to be a robust feature of the model and not to depend on the approximation. On the other hand it is opposite to what is observed in the 3-band model²⁴ where BC stripes constitute the most stable low doping structure.

D. Effect of t' on the stability of stripes

We now proceed to discuss in detail the role of t' on e_h . Due to the dependence of C_K on t' and the constancy of the parameter A we observe in Fig. 5 a shift of optimal stripe filling to smaller values and a steeper minimum upon increasing $|t'|$. Hence, the larger is $|t'|$ the more stable are partially filled stripes with respect to their filled (insulating) counterpart in agreement with the estimate $C_K \sim W \sim |t'|$ and Eq. (8). One can understand the reason for this behavior by comparing the two cases $\nu = 1$ (insulating) and $\nu = 1/2$ (metallic), remembering that the former structure has twice as much holes per stripe. For the sake of simplicity let us neglect for the moment the interaction part C_I . Then, if the cost to create a stripe dominates ($A > C$ or roughly speaking $J > W$), $\nu = 1$ stripes are more convenient because this minimizes the number of stripes that have to be created to accommodate a given number of holes. On the other hand for $\nu = 1$ the Pauli exclusion principle forces to fill the higher kinetic energy states of the active band, which for broad bands becomes energetically unfa-

avorable. As a consequence it is more convenient for systems with broad bands ($W > J$) to pay the energy J in order to create more stripes, thus reducing the filling per stripe and avoiding the occupancy of high kinetic energy states of the active band. Clearly the relevant parameter which controls this behavior is $J/|t'| \sim J/W \sim A/C$ with small ratio A/C favoring partially filled stripes in agreement with Eq. (8) (see also Fig. 6 below). We note that this is in agreement with our findings in the three-band Hubbard model where the role of t' was played by the oxygen-oxygen hopping.²⁴

The energy of (vertical) metallic stripes has to be compared with other saddle-points of the GA energy functional. It should be noted that especially at large doping (but depending also on t'/t) there exists a huge variety of inhomogeneous charge and spin textures which are rather close in energy and compete with the vertical stripe solution. Among this variety we have selected diagonal stripes and spin polarons which energy per hole is reported in Fig. 5b. This choice is motivated by the idea that with increasing kinetic energy the stripes should undergo some kind of melting process which reflects in substantial lateral and orientational fluctuations and an eventual decay into individual segments. However, in our static approach we can only access some 'snapshot' configurations of this melting process and demonstrate the increased degeneracy in energy of these structures with doping.

Two major points result from Fig. 5: *i*) For fixed stripe periodicity d vertical solutions are in general lower in energy than diagonal ones.⁴² However, for larger stripe separation ($d = 5, 6$) and small ratio $|t'/t| \lesssim 0.1$ one observes from Fig. 5 that diagonal and vertical structures are rather close in energy. *ii*) For moderate values of $|t'/t| \lesssim 0.4$ spin polarons are always higher in energy than (vertical) stripe structures but the polaron solution becomes more stable for larger $|t'/t|$ depending on the stripe separation. At low doping where the stripes are almost noninteracting ($d > 5$) the critical value for (vertical) stripe stability is $t'/t \approx -0.4$. In this region of parameters the ground state will have contributions from both stripes and dissociated holes. We can speculate that in this case, going beyond mean-field, stripes will have a more dynamical character. In this sense our finding is in agreement with previous investigations^{40,41} which found a suppression of static stripe formation upon increasing $|t'/t|$. Note that for finite doping the polaronic energy naturally depends on the special arrangement of the self-trapped charge carriers on the lattice. However, for the selected large value of $U/t = 10$ the spin-polarons are quite localized and therefore their energy is almost independent of doping up to hole concentrations $x \approx 0.2$.

Fig. 6 displays the optimal filling ν_{opt} (corresponding to the curve minima in Fig. 5) versus the stripe separation for different next-nearest neighbor hoppings. For stripe distances $d > 4$ the vertical stripes are almost non-interacting and therefore the filling fraction versus t'/t is the same as can be seen from Fig. 6a. For smaller dis-

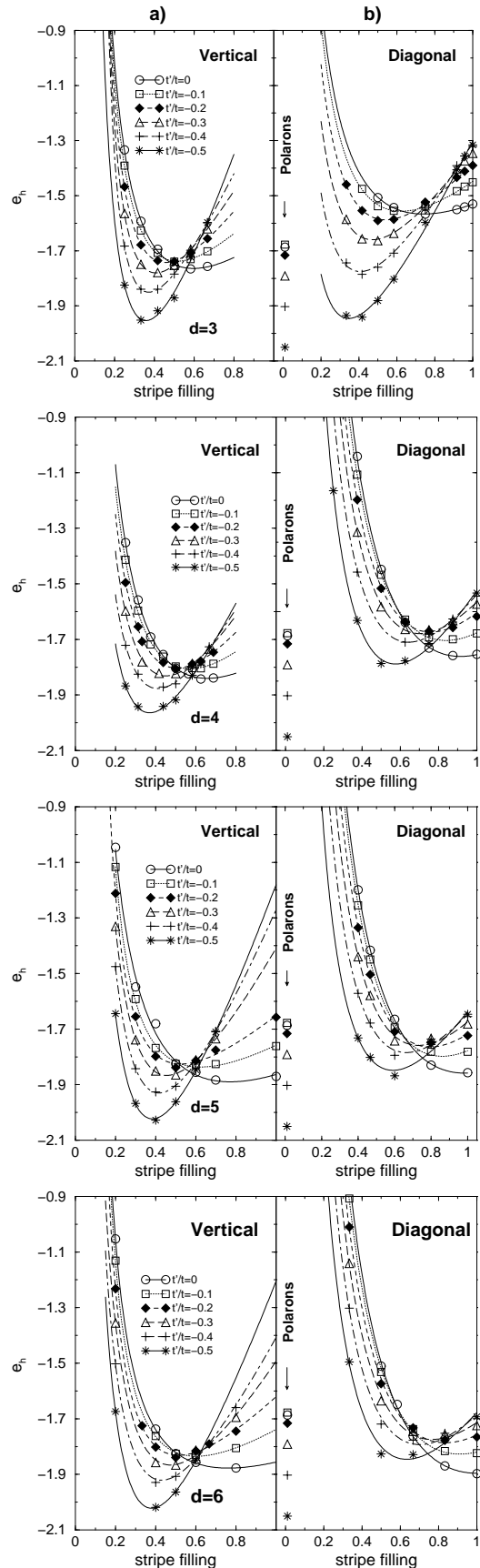


FIG. 5: GA excess energies per hole e_h for vertical SC (a) and diagonal (b) stripes as a function of the stripe filling ν and for various values of t'/t . The stripe separation (in lattice constants) is $d = 3, 4, 5, 6$ (from top to bottom). We also report the energy of the polaron solutions in the right panel.

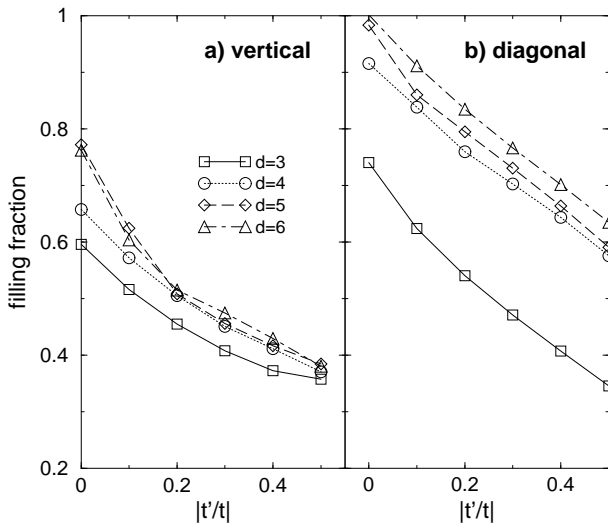


FIG. 6: Optimal stripe filling as a function of periodicity for (a) vertical and (b) diagonal stripes.

tances stripes start to repel, resulting in a shift of e_h to higher values (cf. Fig. 5a). However, the increased inter-stripe interaction leads also to a larger dispersion perpendicular to the stripes which in the e_h curves of Fig. 5 reflects as an increase in curvature (i.e. in the 'kinetic' constant C) upon going from $d = 4$ to $d = 3$ stripes. As a result one therefore observes a shift of ν_{opt} to lower values for the $d = 3$ solution.

The situation for diagonal stripes is qualitatively similar, i.e. upon increasing $|t'/t|$ the minimum of e_h shifts to lower values of ν . Since the kinetic energy in diagonal direction (and thus the parameter C_{diag}) is naturally smaller than along the bonds we find the optimal filling at larger values as compared to vertical stripes. Moreover, diagonal stripes are more extended so that a sizeable inter-stripe interaction is present even for periodicities $d = 5, 6$. In Fig. 5b this reflects as a continuous decrease of the e_h curves upon increasing d . For the same reason ν_{opt} continuously increases with d for fixed t'/t as can be seen from Fig. 6b.

Comparing Fig. 6a with the experimental situation in the LSCO high- T_c compound it thus turns out that the phenomena of half-filled vertical stripes for $d \geq 4$ requires for the ratio between next-nearest and nearest neighbor hopping $t'/t \approx -0.2$. For this value Fig. 7 reports the corresponding e_h curves but now plotted as a function of the hole doping. Since the charge modulation of vertical stripes has a width of about 4-5 lattice constants the inter-stripe interaction is vanishingly small for $d \geq 5$ and thus the energy depends only weakly on distance. Moreover, from Fig. 5 we have seen that in this regime the ground state solution has always filling close to $\nu = 1/2$ and thus the incommensurability

$$\epsilon = \frac{x}{2\nu}. \quad (9)$$

behaves as $\epsilon \approx x$ in agreement with experiment.^{3,4,5,6} For $d \leq 4$ ($x \geq 1/8$) stripes overlap (see Fig. 1) which leads to a vertical shift of the curves as shown in Fig. 7a. Hence it is unfavorable for the system to increase the density of stripes from $d = 4$ to $d = 3$, the incommensurability gets locked at $\epsilon = 1/8$ ($d = 4$) and the filling ν of the stripes starts to increase. This feature favors the degeneracy between bond and site centered vertical stripes as can be deduced from Fig. 4b suggesting the importance of lateral stripe fluctuations in this doping range. Disregarding for the moment the polaron solution we observe a further transition toward $d = 3$ stripes at $x \sim 0.2$. A similar result has been found also in the 3-band model.²⁴

Diagonal stripes are more extended so that the corresponding e_h curves start to shift for $d \leq 5$ already. In the low doping regime they are less stable than vertical stripes, however, the energy difference becomes rather small for $x \gtrsim 0.2$. Moreover, both vertical and diagonal stripe solutions approach the energy of the polaron solution at this particular doping. This means that for concentrations $x > 0.2$ the energy is almost independent of the charge topology. The GA landscape is not dominated by a well defined saddle point and an associated Slater determinant but a large number of energy minima with very different charge topologies compete. In this regime the ground state will thus have contributions from all Slater determinants corresponding to the different charge configurations with equivalent energy. We expect a state which has lost the orientational order information.⁵¹

In the low doping regime neutron scattering experiments on LSCO observe a change of the incommensurability vector below $x \approx 0.05$ from the vertical to the diagonal direction.^{4,12,13} From the results as shown in Fig. 7 we cannot infer a crossover towards diagonal solutions at low doping. However, the closeness in energy of vertical and diagonal structures suggests that the orthorhombic distortion, which continuously increases upon underdoping in LSCO may lead to a stabilization of the diagonal stripe phase at small hole concentrations (see Normand et al.⁵³ for a detailed discussion of the relation between stripe orientation and lattice distortion). Moreover, we believe that other effects, not included in our model, are important in this regard. Indeed the contribution of long-range Coulomb interactions is expected to become important at low doping. A point charge estimate shows that this tends to favor diagonal configurations over vertical ones.

To summarize the results for $t'/t = -0.2$: We obtain half-filled vertical stripes and $\epsilon = x$ up to hole concentrations $x = 1/8$ and increasing ν and $\epsilon = 1/8$ for $1/8 < x < 0.2$ in agreement with experiment^{3,4,5,6} and with our previous 3-band computations.²⁴ The behavior for the filling implies that the chemical potential μ will be approximately constant for $x < 1/8$ and decrease with doping for $x > 1/8$ which is also supported by experiment.^{26,27} However, it should be noted that the theoretically obtained shift in μ exceeds the experimen-

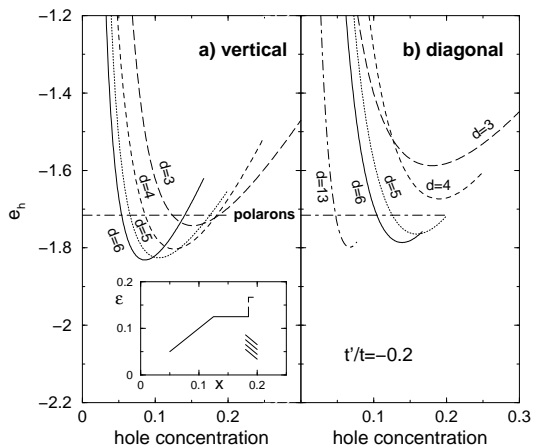


FIG. 7: Energies per hole for vertical (a) and diagonal (b) stripes as a function of doping. $t'/t = -0.2$ as appropriate for LSCO. The inset displays the incommensurability versus doping as deduced from (a). The diagonal pattern indicates the degeneracy with diagonal stripes.

tal one by a factor of 2...3 which may be attributed to finite size effects. A similar discrepancy is also observed in the 3-band model and we refer to Ref. 24 for a further discussion of this point.

Finally, in Fig. 8 we show the phase diagram calculated for $t'/t = -0.4$ which is considered to be the appropriate ratio for the $\text{Tl}_2\text{Ba}_2\text{Ca}_2\text{Cu}_3\text{O}_{10}$ and $\text{HgBa}_2\text{CaCu}_2\text{O}_6$ compounds.³⁶ In this case low doping vertical stripes have a filling fraction of $\nu \approx 0.4$ so that the incommensurability $\epsilon \approx 1.25x$ is expected to grow faster than for the LSCO compounds. However, already the $d = 4$ structures are unstable with respect to the spin polaron solution and thus the incommensurability starts to saturate for $x \geq 0.08$ corresponding to the $d = 5$ structure. Moreover since the polaron solution is rather close in energy a static stripe phase is quite unlikely to exist in Tl- (Hg-) based cuprates. It is rather more meaningful to have in mind a picture where stripes appear as snapshots in the dynamical evolution of the system. In this context it is interesting to observe that for all dopings diagonal stripes are higher in energy than the polaron structure. The low doping phase may resemble that of a 'stripe nematic'⁵¹ where orientational symmetry is broken but quantum fluctuations mainly lead to a restoration of translational symmetry.

IV. CONCLUSIONS

Within the inhomogeneous GA we have investigated metallic stripe states in the one-band extended Hubbard model for a fixed value of the on-site repulsion $U/t = 10$ as appropriate for the cuprates. Metallic stripes were shown to be favored by a negative t'/t and the physics of this behavior has been clarified in terms of the competition between the kinetic energy along the stripe and

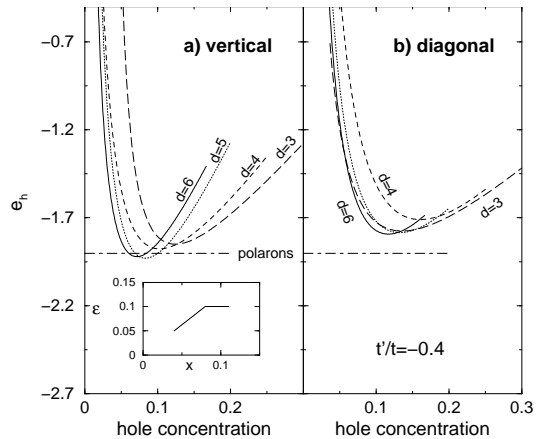


FIG. 8: Energies per hole for vertical (a) and diagonal (b) stripes as a function of doping. $t'/t = -0.4$ as appropriate for Bi2212. The inset displays the incommensurability versus doping as deduced from (a).

the creation energy of a stripe. In this regard the HF approximation has been shown to lead to gross quantitative and often qualitative errors.

Generally the present results are in agreement with our previous findings in the 3-band model, in particular the behavior of the incommensurability and the chemical potential, showing that our previous results in the 3-band model are quite robust²⁴. On the other hand there are also important differences. In the present model SC stripes are more stable at low doping as compared to BC stripes. This is in agreement with DMFT computations³⁷ and therefore seems to be a robust feature of the one-band model and not to depend on the approximation.

One should keep in mind that effective models, like the one-band Hubbard model, are in principle designed for the description of electronic excitations in a diluted, uniform phase. Usually it is not guaranteed that they will give correct results when one compares the relative stability of dense non-uniform phases.⁵⁵ Therefore we consider the 3-band result for the stripe state symmetry as more reliable for the description of real cuprates than the one-band calculation. Further support to this conclusion comes from the analysis of transport data.^{28,29} Indeed within the 3-band Hamiltonian where BC stripes constitute the most stable low doping state we have explained²⁴ an anomalous vanishing of the transport coefficients^{28,29} as due to the particular band structure of BC stripes which turns out to be particle-hole symmetric close to the Fermi level. Since the band structure of half-filled SC stripes is not particle-hole symmetric around the Fermi level (cf. Fig. 2) the one-band model cannot account for the observed vanishing of transport coefficients.^{28,29}

When the next-nearest neighbor hopping is fixed to $t'/t = -0.2$ stripes turn out to be half-filled at low doping. The behavior of the incommensurability and chemical potential is in good agreement with experiment in LSCO. Our investigation therefore supports the LDA

based one band-mapping of Ref. 36 where a similar value for the next-nearest neighbor hopping has been reported for LSCO materials.

As doping increases the energy becomes independent of the charge topology. SC vertical, BC vertical, diagonal stripes and a polaron lattice all become degenerate. We associate this with a transition from a state with orientational order to an isotropic state.⁵¹ This quantum melting of the stripe state for $x > 0.2$ is also reminiscent of the existence of a quantum critical point in the slightly overdoped regime as has been proposed by Castellani *et al.*⁵⁴

Since stripes are charged the lateral motion of stripes is optically active. Therefore the decrease in the energy gap between SC and BC stripes should reflect in the softening of an optically active electronic mode. We have explicitly shown this behavior in a GA+RPA computation in the three-band model where the softening of a stripe phason³² can explain the shift of the mid-infrared peak in optical conductivity experiments on LSCO.^{33,34} We expect a similar behavior in the charge response of

the one-band model.

Our present results allow for predictions for other cuprate families. For larger values of $|t'|$ we obtain lower values of ν . Therefore according to Eq. (9) we predict a steeper curve of ϵ vs. x for small x in Tl and Hg based compounds. As $|t'|$ increases we also find that the relative stability of stripes with respect to isolated polarons decreases. This loss of stability may indicate that stripes have a more dynamical character in these materials.

Having in mind the differences and similarities between the one-band and the three-band description one can still obtain very useful qualitative information from the one-band description. Since within the present work we have set up the relevant parameter set and stable stripe saddle-points for the LSCO compounds this represents the first step for an investigation of the associated charge and spin dynamics. Further on the one-band model allows for the investigation of larger clusters and thus the structure of these excitations in q-space can be investigated in more detail than possible within the 3-band Hamiltonian. Work in this direction is in progress.

-
- ¹ J. M. Tranquada, B. J. Sternlieb, J. D. Axe, Y. Nakamura and S. Uchida, *Nature* **375**, 56 (1995).
- ² J. M. Tranquada, J. D. Axe, N. Ichikawa, Y. Nakamura, S. Uchida, and B. Nachumi, *Phys. Rev. B* **54**, 7489 (1996).
- ³ J. M. Tranquada, J. D. Axe, N. Ichikawa, A. R. Moodenbaugh, Y. Nakamura, and S. Uchida, *Phys. Rev. Lett.* **78**, 338 (1997).
- ⁴ K. Yamada, C. H. Lee, K. Kurahashi, J. Wada, S. Wakimoto, S. Ueki, H. Kimura, Y. Endoh, S. Hosoya, G. Shirane, R. J. Birgeneau, M. Greven, M. A. Kastner, and Y. J. Kim, *Phys. Rev. B* **57**, 6165 (1998).
- ⁵ M. Arai, T. Nishijima, Y. Endoh, T. Egami, S. Tajima, K. Tomimoto, Y. Shiohara, M. Takahashi, A. Garrett, and S. M. Bennington, *Phys. Rev. Lett.* **83**, 608 (1999).
- ⁶ M. Arai, Y. Endoh, S. Tajima, and S. M. Bennington, *Int. J. Mod. Phys. B* **14**, 3312 (2000).
- ⁷ S. M. Hayden, G. H. Lander, J. Zarestky, P. J. Brown, C. Stassis, P. Metcalf, and J. M. Honig, *Phys. Rev. Lett.* **68**, 1061 (1992).
- ⁸ C. H. Chen, S-W. Cheong and A. S. Cooper, *Phys. Rev. Lett.* **71**, 2461 (1993).
- ⁹ J. M. Tranquada, D. J. Buttrey, V. Sachan, and J. E. Lorenzo, *Phys. Rev. Lett.* **73**, 1003 (1994).
- ¹⁰ P. Dai, H. A. Mook, R. D. Hunt, and F. Dogan, *Phys. Rev. B* **63**, 054525 (2001).
- ¹¹ H. A. Mook, P. Dai, and F. Dogan, *Phys. Rev. Lett.* **88**, 097004 (2002).
- ¹² M. Matsuda, M. Fujita, K. Yamada, R. J. Birgeneau, M. A. Kastner, H. Hiraka, Y. Endoh, S. Wakimoto, and G. Shirane, *Phys. Rev. B* **62**, 9148 (2000).
- ¹³ M. Fujita, K. Yamada, H. Hiraka, P. H. Gehring, S.H. Lee, S. Wakimoto, and G. Shirane, *Phys. Rev. B* **65**, 064505 (2002).
- ¹⁴ H. He, Y. Sidis, P. Bourges, G. D. Gu, A. Ivanov, N. Koshizuka, B. Liang, C. T. Lin, L. P. Regnault, E. Schoenher, and B. Keimer, *Phys. Rev. Lett.* **86**, 1610 (2001).
- ¹⁵ H. A. Mook, F. Dogan, and B. C. Chakoumakos, *cond-mat/9811100, Stripes and Related Phenomena*, eds. A. Bianconi and N. L. Saini, Kluwer Academic (2000).
- ¹⁶ S. Krämer and M. Mehring, *Phys. Rev. Lett.* **83**, 396 (1999).
- ¹⁷ P. M. Singer, A. W. Hunt, and T. Imai, *Phys. Rev. Lett.* **88**, 047602 (2002).
- ¹⁸ J. Haase, C. P. Slichter, and C. T. Milling, *J. Supercond.* **15**, 339 (2002).
- ¹⁹ J. Zaanen and O. Gunnarsson, *Phys. Rev. B* **40**, 7391 (1989).
- ²⁰ K. Machida, *Physica C* **158**, 192 (1989).
- ²¹ H. J. Schulz, *Phys. Rev. Lett.* **64**, 1445 (1990).
- ²² D. Poilblanc and T. M. Rice, *Phys. Rev. B* **39**, 9749 (1989).
- ²³ S-W. Cheong, G. Aeppli, T. E. Mason, H. Mook, S. M. Hayden, P. C. Canfield, Z. Fisk, K. N. Clausen, and J. L. Martinez *Phys. Rev. Lett.* **67**, 1791 (1991).
- ²⁴ J. Lorenzana and G. Seibold, *Phys. Rev. Lett.* **89**, 136401 (2002).
- ²⁵ M. C. Gutzwiller, *Phys. Rev.* **137**, A1726 (1965).
- ²⁶ A. Ino, T. Mizokawa, A. Fujimori, K. Tamasaku, H. Eisaki, S. Uchida, T. Kimura, T. Sasagawa, and K. Kishio, *Phys. Rev. Lett.* **79**, 2101 (1997).
- ²⁷ N. Harima, J. Matsuno, A. Fujimori, Y. Onose, Y. Taguchi, and Y. Tokura, *Phys. Rev. B* **64**, R220507 (2001).
- ²⁸ T. Noda, H. Eisaki and S. Uchida, *Science* **286**, 265 (1999).
- ²⁹ Yayu Wang and N. P. Ong, *Proc. Natl. Acad. Sci. U.S.A* **98**, 11091 (2001).
- ³⁰ J. Lorenzana and C. Castellani and C. Di Castro, *Europhys. Lett.* **57**, 704 (2002).
- ³¹ G. Seibold and J. Lorenzana, *Phys. Rev. Lett.* **86**, 2605 (2001).
- ³² J. Lorenzana and G. Seibold, *Phys. Rev. Lett.* **90**, 066404 (2003).
- ³³ S. Uchida, T. Ido, H. Takagi, T. Arima, Y. Tokura, and S. Tajima, *Phys. Rev. B* **43**, 7942 (1991).
- ³⁴ M. Suzuki, *Phys. Rev. B* **39**, 2312 (1989).
- ³⁵ A. K. McMahan, J. F. Annett, and R. M. Martin, *Phys.*

- Rev. B **42**, 6268 (1990).
- ³⁶ E. Pavarini, I. Dasgupta, T. Saha-Dasgupta, O. Jepsen, and O. K. Andersen Phys. Rev. Lett. **87**, 047003 (2001).
- ³⁷ Marcus Fleck, Eva Pavarini and Ole Krogh Andersen, cond-mat/0102041.
- ³⁸ K. Machida and M. Ichioka, J. Phys. Soc. Jpn. **68**, 2168 (1999).
- ³⁹ B. Valenzuela, M. A. H. Vozmediano, and F. Guinea, Phys. Rev. B **62**, 11312 (2000).
- ⁴⁰ B. Normand and A. P. Kampf, Phys. Rev. B **65**, 020509 (2001).
- ⁴¹ M. Fleck and A. I. Lichtenstein and A. M. Oleś, Phys. Rev. B **64**, 134528 (2001).
- ⁴² Note that we have defined the distance d for diagonal stripes as the spacing in *vertical* direction.
- ⁴³ M. Inui and P. B. Littlewood, Phys. Rev. B **44**, 4415 (1991).
- ⁴⁴ M. S. Hybertsen, E. B. Stechel, W. M. C. Foulkes, and M. Schlüter, Phys. Rev. B **45**, 10032 (1992).
- ⁴⁵ G. Seibold, E. Sigmund, and V. Hizhnyakov, Phys. Rev. B **57**, 6937 (1998).
- ⁴⁶ E. Dagotto, Rev. Mod. Phys. **66**, 763 (1994).
- ⁴⁷ F. Gebhard, Phys. Rev. B **41**, 9452 (1990).
- ⁴⁸ G. Kotliar and A. E. Ruckenstein, Phys. Rev. Lett. **57**, 1362 (1986).
- ⁴⁹ A. Sadori and M. Grilli, Phys. Rev. Lett. **84**, 5375 (2000).
- ⁵⁰ I. Martin, G. Ortiz, A. V. Balatsky, and A. R. Bishop, Int. J. Mod. Phys. B **14**, 3567 (2000).
- ⁵¹ S. A. Kivelson, E. Fradkin, and V.J. Emery, Nature **393**, 550 (1998).
- ⁵² M. Fleck, A. I. Lichtenstein, Eva Pavarini, and A. M. Oleś, Phys. Rev. Lett. **84**, 4962 (2000).
- ⁵³ B. Normand and A. P. Kampf, Phys. Rev. B **64**, 024521 (2001).
- ⁵⁴ C. Castellani, C. Di Castro, and M. Grilli, Phys. Rev. Lett. **75**, 4650 (1995).
- ⁵⁵ J. van den Brink, M. B. J. Meinders, J. Lorenzana, R. Eder, and G. A. Sawatzky, Phys. Rev. Lett. **75** 4658 (1995).